Journal of Oral Biosciences 61 (2019) 55–63

Contents lists available at ScienceDirect

Journal of Oral Biosciences

journal homepage: www.elsevier.com/locate/job

Three-dimensional configuration of apical epithelial compartments including stem cell niches in guinea pig cheek teeth

Yuta Seino [a], Mitsushiro Nakatomi [b], Hiroko Ida-Yonemochi [a], Daisuke Koga [c], Tatsuo Ushiki [d], Hayato Ohshima [a,*]

[a] Division of Anatomy and Cell Biology of the Hard Tissue, Department of Tissue Regeneration and Reconstruction, Niigata University Graduate School of Medical and Dental Sciences, 2-5274 Gakkocho-dori, Chuo-ku, Niigata 951-8514, Japan
[b] Division of Anatomy, Department of Health Improvement, Kyushu Dental University, 2-6-1 Manazuru, Kokurakita-ku, Kitakyushu 803-8580, Japan
[c] Department of Microscopic Anatomy and Cell Biology, Asahikawa Medical University, 2-1-1-1 Midorigaoka Higashi, Asahikawa 078-8510, Japan
[d] Division of Microscopic Anatomy and Bio-imaging, Department of Cellular Function, Niigata University Graduate School of Medical and Dental Sciences, 1-757 Asahimachi-dori, Chuo-ku, Niigata 951-8510, Japan

ARTICLE INFO

Article history:
Received 21 October 2018
Received in revised form
4 January 2019
Accepted 11 January 2019
Available online 21 January 2019

Keywords:
Epithelial cell
Guinea pig
Molar
Stem cell
Three-dimensional imaging

ABSTRACT

Objectives: Continuously growing rodent incisors have an apically located epithelial stem cell compartment, known as an "apical bud" (AB). Few studies have described the morphological features of ABs and stem cell niches in continuously growing premolars/molars. We attempted to clarify the relationship between the three-dimensional configuration of ABs and the stem cell niches in guinea pig cheek teeth.
Methods: We perfusion-fixed four-week-old guinea pigs, then decalcified their premolars/molars to produce serial paraffin sections, which we immunostained for Sox2. We reconstructed the serial sections using image processing and analysis software. We processed undecalcified samples for scanning electron microscopy by KOH digestion.
Results: Two types of epithelia with M and Δ shapes surrounded the S-shaped dental papilla in the apical region of the premolars/molars, and there were three Sox2-positive epithelial bulges above the M- and Δ-shaped epithelia. Sox2-positive epithelial stem cell niches were restricted to the apical side, and cell proliferation and differentiation immediately proceeded in the crown-analogue dentin. The Sox2-positive epithelial stem cell niches were sparsely distributed and extended to the occlusal side. We also detected continuously proliferating cells in the cervical loop and Hertwig's epithelial root sheath of the root-analogue dentin.
Conclusions: Our findings suggest that guinea pig cheek teeth have three ABs, and the complex configuration of these types of teeth may be attributed to the prompt formation of crown-analogue dentin followed by the long-term formation of root-analogue dentin.

1. Introduction

Tooth development proceeds via epithelial–mesenchymal interactions in the following sequential steps: determination of tooth-forming regions, initiation of tooth formation, determination of tooth shape, and regulation of tooth renewal. For the most part, the same molecular pathways are iteratively used throughout the various stages of tooth development; the transforming growth factor β (TGFβ), fibroblast growth factor (FGF), sonic hedgehog (SHH), and WNT signaling pathways are repeatedly involved during the process [1–3]. Tooth configuration is determined by the enamel–dentin junction during tooth morphogenesis, suggesting that tooth morphology is elaborated by dental epithelial cell proliferation and differentiation. In reality, the dental epithelium and mesenchyme determine the cusp size and tooth size, respectively, and the cusp number is coregulated by the tooth size and cusp size. The mesenchymal cell number does not determine the tooth size but does determine the number of teeth [4]. Furthermore, a recent study clearly demonstrated that the shape of the cusps is determined by the dental epithelium at the cap stage, and the cellular geometry in the inner enamel epithelium is correlated with the shape of the cusps [5]. However, the mechanisms that regulate the precise epithelial cell proliferation and differentiation that determine various tooth morphologies have not been thoroughly elucidated to date.

The basal mammalian dentition consists of several tooth types: incisors, canines, premolars, and molars. Of these tooth types, the premolars and molars have evolved the greatest complexity,

* Corresponding author.
E-mail address: histoman@dent.niigata-u.ac.jp (H. Ohshima).

https://doi.org/10.1016/j.job.2019.01.002
1349-0079/

especially in mammals that specialize in eating fibrous vegetation [6]. The elaboration of many kinds of cusp patterns can be explained by the activator–inhibitor theory [7,8]. The most frequently observed evolutionary solution to mammalian tooth loss due to wear is the development of high crowned (hypsodont) and continuously growing (hypselodont) teeth. The homeostasis of continuously growing teeth is maintained by both tooth growth due to the continuous supply of enamel- and dentin-forming progenitor cells, and attrition of the incisal edge. Rodent incisors are the typical model for continuously growing teeth. All stages of odontogenesis (amelogenesis and dentinogenesis) can be observed if sagittal sections of a tooth are prepared. The labial dentin (referred to as crown-analogue) is covered with enamel, whereas cross-sections of the lingual side (referred to as root-analogue) contain cementum [9,10]. Continuously growing rodent incisors have an epithelial stem cell compartment referred to as an "apical bud" (AB) [11–13] or a "cervical loop" (CL) in the apical end. The stem cell niche in the AB was first identified when label-retaining cells were found to be localized inside the stellate reticulum [14,15], and this has been corroborated more recently by *in vivo* genetic lineage tracing [16,17]. In contrast, there is little data regarding the morphological features of ABs and stem cell niches in continuously growing premolars/molars.

Continuously growing teeth are represented not only in rodent incisors but also in the premolars/molars of certain species, including rabbits, guinea pigs, and voles [18–20]. Sox2 marks the incisor stem cells, and Sox2-expressing cells contribute not only to the formation of ameloblasts but also to the formation of all other epithelial cell lineages of the tooth [16]. The AB resembles other stem cell niches, such as the crypts of the intestine and the bulge of the hair follicle. All of these niches are surrounded by mesenchymal tissue, which provides cues to the epithelium that are necessary for the self-renewal and differentiation of epithelial cells. In the present study, we investigated the relationship between the three-dimensional configuration of the ABs and stem cell niches in guinea pig cheek teeth using reconstructed serial paraffin sections, Sox2 immunohistochemistry, and scanning electron microscopy (SEM) with KOH digestion.

2. Materials and methods

2.1. Tissue preparation

All animal experiments complied with the guidelines by the Ministry of Education, Culture, Sports, Science and Technology, the Ministry of the Environment, and the Science Council of Japan and were carried out in accordance with the Act on Welfare and Management of Animals. We placed two 4-week-old male Hartley guinea pigs under deep anesthesia by intraperitoneal injection of chloral hydrate (350 mg/kg). We then perfused the guinea pigs with physiological saline followed by 4% paraformaldehyde in a 0.1 M phosphate buffer (pH 7.4). We removed the maxillae and mandibles *en bloc* and separated them into right and left sides. We then decalcified each jaw in a 10% ethylenediaminetetraacetic acid disodium salt (EDTA-2Na) solution for 4 weeks at 4 °C for immunohistochemical analysis. We dehydrated the EDTA-2Na-decalcified samples and embedded them in paraffin. Subsequently, we cut the samples into 4-μm serial sections and mounted them on Matsunami adhesive silane (MAS)-coated glass slides (Matsunami Glass, Osaka, Japan). We stained some of the sections with hematoxylin and eosin (H&E).

2.2. Immunohistochemistry

We performed immunohistochemical analyses using the avidin–biotin peroxidase complex (ABC) (Vectastain ABC kit; Vector Laboratories, Inc, Burlingame, CA, USA) method. We autoclaved the specimens for 5 min at 121 °C in the presence of citrate buffer (0.01 M, pH 6.0), then washed them with 0.05 M Tris–HCl buffer (pH 7.4). Next, we treated the samples with 0.3% hydrogen peroxide in methanol for 30 min at 24 °C to block endogenous peroxidase activity, and incubated them overnight at 4 °C with anti-Sox2 mouse IgG primary antibody (Sox-2 E-4: sc-365823, Santa Cruz Biotechnology, Inc, Dallas, TX, USA) diluted at a ratio of 1:25 with 0.01 M phosphate-buffered saline (PBS) containing 0.05% Triton X-100. We also incubated the sections with biotinylated anti-mouse IgG (Vector Laboratories) diluted at a ratio of 1:100 with PBS for 60 min at 24 °C, then further incubated them with Vectastain ABC reagent for 60 min at 24 °C. To visualize the reaction products, we treated the sections with 0.02% 3,3′-diaminobenzidine (Dohjin Laboratories, Kumamoto, Japan) in 0.05 M Tris–HCl buffer (pH 7.4) containing 0.005% hydrogen peroxide, and counterstained them with hematoxylin.

2.3. SEM

We transcardially perfused one of the guinea pigs with PBS followed by 2.5% glutaraldehyde in 0.06 M cacodylate buffer (pH 7.4) containing 0.5% sucrose. We immersed the maxillae and mandibles in the same fixative for an additional 12 h. We then removed the premolars and molars from the jaws, and removed the extracellular matrices including collagen components and intercellular substances by KOH digestion [21]. We immersed the tissues in 30% KOH for 8 min at 62–65 °C and washed them several times in 0.1 M phosphate buffer. We stained the specimens according to the tannin–osmium method by treating them with a 1% tannic acid solution and 1% OsO_4, dehydrated in a graded ethanol series. We then transferred the specimens to isoamyl acetate for 10–30 min and dried them in a critical-point dryer (HCP-1, Hitachi, Tokyo, Japan) using liquid CO_2. We mounted the dried tissues on metal stubs, coated them with platinum–palladium using an ion-coater (IB-3, Eiko, Tokyo, Japan), and examined them by SEM (S-2380N, Hitachi, Tokyo, Japan) at an accelerating voltage of 10 kV.

2.4. Three-dimensional (3D) reconstruction

We generated a 3D reconstruction of Sox2 expression from serial horizontal 4-μm sections. The pictures were imported into a stack via graphical software (Photoshop CC: Adobe Systems Incorporated, CA, USA). We aligned the individual pictures using the epithelial boundary as a reference. We manually traced the shape of the epithelium; we filled this subpath with white on a black layer. We resliced the aligned pictures as sagittal sections using Fiji software (ver. 10.2; National Institutes of Health, MD, USA). We have described the procedures in detail in a previous report [12]. We superimposed the 3D images of the epithelium and Sox2 expression and selected the frontal, sagittal, and tilted projections for presentation.

3. Results

3.1. Comparison between a mouse incisor and a guinea pig premolar/molar

Fig. 1 depicts a mouse mandible with an incisor and three molars, and a guinea pig mandible with a premolar and three molars (see also Supplementary data 1-4). The mouse incisor has a banana-like shape with an AB in the apical end. The labial dentin is covered with enamel (crown-analogue dentin) and the lingual side is covered in cementum (root-analogue dentin). A cross section of the tooth reveals one circular cusp located on the labial side (Fig. 1A, B).

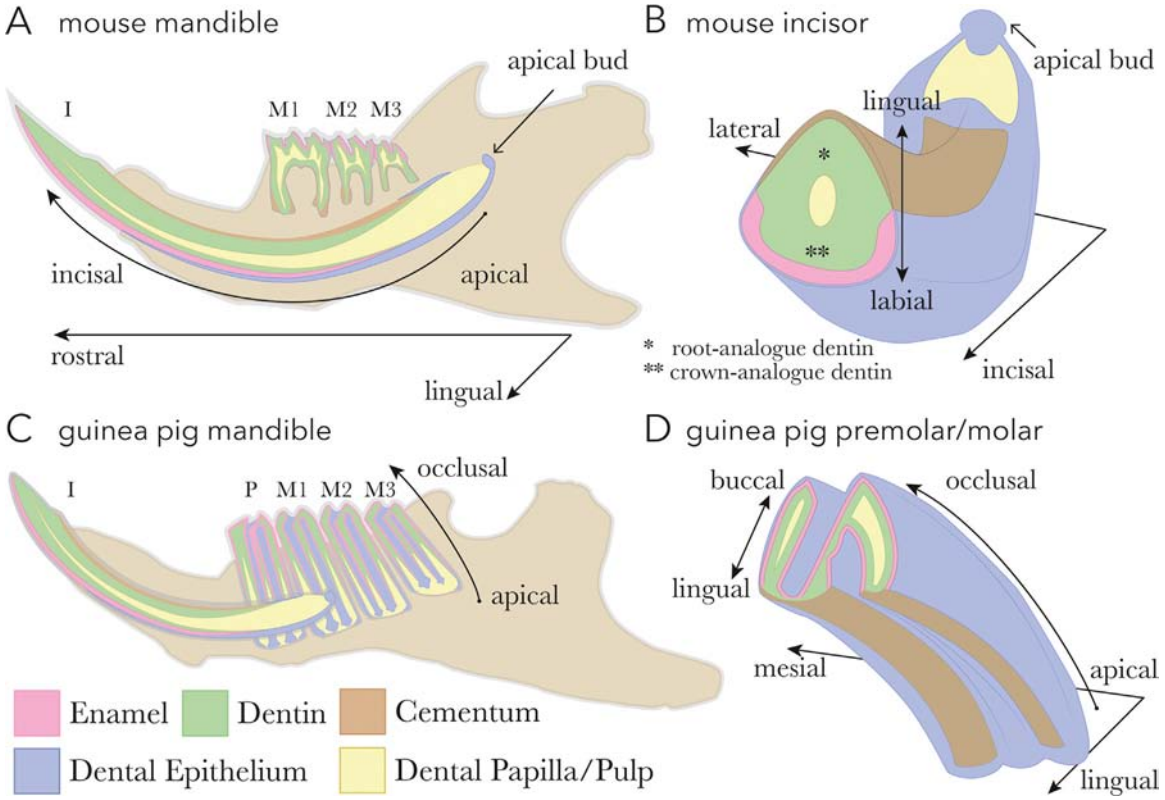

Fig. 1. The structures of mouse and guinea pig mandibles and teeth. The figure illustrates 2D views of a mouse mandible with an incisor and three molars (A) and a guinea pig mandible with an incisor, a premolar, and three molars (C), and 3D views of a mouse incisor (B) and a guinea pig premolar/molar (D), where the incisal edge (B) or occlusal surface (D) has been transversely trimmed. (A, B) The mouse incisor has a banana-like shape with an apical bud in the apical end (arrows). The labial dentin is covered with enamel (crown-analogue dentin) and the lingual side is covered with cementum (root-analogue dentin). (C, D) The guinea pig premolar/molar has unique features: a longitudinal, deeply folded groove on each buccal or lingual side; all surfaces of the dentin are covered with enamel except the lingual side (root-analogue side). I, incisor; M1, first molar; M2, second molar; M3, third molar; P, premolar.

Supplementary material related to this article can be found online at https://doi.org/10.1016/j.job.2019.01.002.

Guinea pig premolar/molars have unique features: a longitudinal, deeply folded groove on each buccal or lingual side, covering all surfaces of the dentin except the buccal side of the uppers and the lingual side of the lowers (root-analogue side). The morphology of the premolars/molars of the uppers is opposite to that of the lowers. A cross section of the tooth reveals two conical cusps on the crown-analogue side and one enamel groove on the root-analogue side (Fig. 1C, D). We have described the detailed configuration of guinea pig premolars/molars in a previous report [20].

3.2. SEM

SEM with KOH digestion revealed the 3D features of the epithelial components in the apical end of the premolars/molars. In the present analysis, the mesenchymal tissue became detached from the dentin matrix owing to the loss of predentin, although the epithelial components are easily broken during sample preparation. The S-shaped mesenchymal tissue was surrounded by the epithelium, the buccal (in the mandibular teeth) and lingual (in the maxillary teeth) sides of which were broken and did not appear. Nevertheless, we succeeded in observing the precise 3D configuration of the central part of the apical epithelium (Fig. 2A-C). Furthermore, we were able to determine the 3D relationships among the inner enamel epithelium (IEE), ameloblasts, enamel, dentin, odontoblasts, and dental pulp (Fig. 2D, E).

3.3. Sox2 immunohistochemistry

When we examined the Sox2-immunostained serial sections from the apical end in the direction of occlusion (Fig. 3), intense staining first appeared in the epithelial components (mesial AB) of the crown-analogue side (Fig. 3A), and this immunopositive reaction extended throughout the IEE (Fig. 3B). More intense staining appeared in the epithelial components (distal AB) of the crown-analogue side (Fig. 3C), and this reaction also extended throughout the IEE (Fig. 3D, E). Subsequently, an additional intense Sox2-immunopositive epithelial island (lingual AB in the mandible or buccal AB in the maxilla) appeared on the root-analogue side (Fig. 3F), and the boundary of this island continued to react intensely. Sox2-immunoreactivity gradually decreased in intensity on the crown-analogue side, and the cervical loops (CLs) remained immunostained, even as the sections approached the occlusal side (Fig. 3G). Four Hertwig's epithelial root sheaths (HERS)—where Sox2-positive cells intermingled with Sox2-negative cells—elongated mesiodistally from the mesial CL, the island CLs, and the distal CL to combine, resulting in the establishment of an epithelial covering surrounding the dental papilla on the root-analogue side (Fig. 3H, I). The intensity of Sox2-immunoreactivity in each section varied according to its inclination.

3.4. 3D reconstruction

The 3D reconstruction of serial Sox2-immunostained sections clearly demonstrated the 3D configuration of the complex apical epithelial tissues in combination with Sox2-immunoreactivity (Fig. 4, Supplementary data 5). The apical epithelial components of

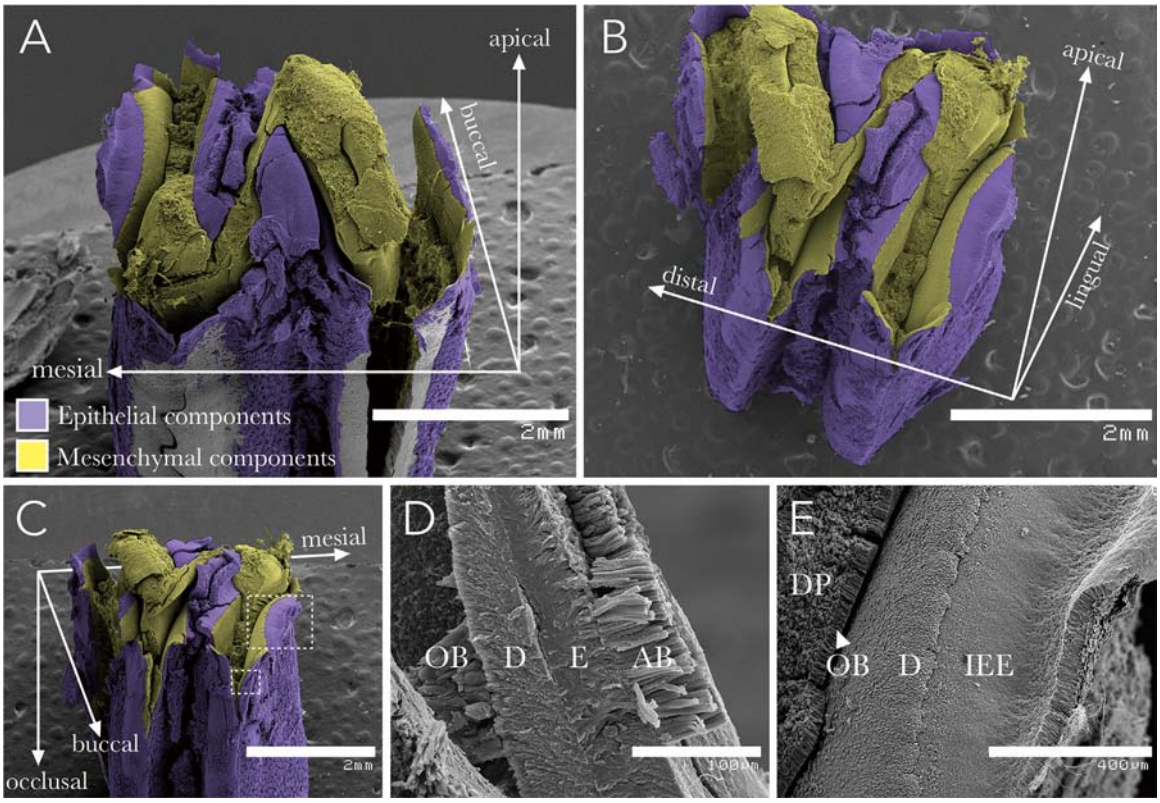

Fig. 2. Scanning electron microscope images of a mandibular molar. The figure comprises scanning electron microscope images, obtained using the KOH digestion method, that represent 3D features of epithelial components in the apical end of a mandibular molar. (A-C) The S-shaped mesenchymal tissue (yellow) is surrounded by the epithelium (purple), the buccal side of which is broken (not visible). (D, E) The 3D relationships among the inner enamel epithelium (IEE), ameloblasts (AB), enamel (E), dentin (D), odontoblasts (OB), and dental pulp (DP) are visible. Figures D and E are higher-magnification views of the boxed areas in C. Bars = 2 mm (A-C), 400 μm (E), 100 μm (D). (For interpretation of the references to color in this figure legend, the reader is referred to the web version of this article).

the premolars/molars showed the combined features of the M-shape on the crown-analogue side and the Δ-shape on the root-analogue side. Two epithelial bulges (mesial and distal ABs) were located near the tops of the M-shaped epithelium, and a large mushroom-like epithelial prominence was visible in the valley of the M-shape. Furthermore, a Δ-shaped epithelial island appeared near the valley of the M-shaped epithelium, so that the S-shaped dental papilla was surrounded by M- and Δ-shaped epithelia on the crown- and root-analogue sides, respectively. The Sox2-positive reactions represented the combined features of the M- and Δ-shapes that corresponded to the ABs and IEE, and the HERSs and other components such as the stratum intermedium (SI), stellate reticulum (SR), and outer enamel epithelium (OEE) of the enamel organ showed evidence of disperse Sox2-positive reactions.

Supplementary material related to this article can be found online at https://doi.org/10.1016/j.job.2019.01.002.

4. Discussion

4.1. Configuration of the apical epithelium of guinea pig premolars/molars

The common method used to examine the 3D configuration of the epithelium is by direct observation using SEM after the mesenchyme has been stripped from it. We succeeded in elucidating the 3D morphology of the ABs of mouse incisors using this method [11]. However, the application of this method to the apical epithelium of guinea pig premolars/molars does not ensure retention of the *in vivo* configuration owing to the complex morphology of the S-shaped mesenchyme (dental papilla) and the epithelium with its mushroom-like prominence. To overcome this problem, we used KOH digestion [21] to improve the SEM examination of the guinea pig epithelia. This method completely removes collagen fibers while preserving elastic fibers and other cellular elements in their original shapes and locations. The present study demonstrates that the 3D relationship between ameloblasts, enamel, dentin, and odontoblasts is visible using this method. Furthermore, unmineralized predentin, which comprises collagen fibers, is removed by KOH digestion, allowing the mesenchymal tissues to be stripped from the dentin matrix, thereby exposing the epithelial components. We were unable to avoid the breakdown of the epithelial components during sample preparation owing to the peculiar morphological features of guinea pig teeth mentioned above. Nevertheless, this method revealed the precise morphological configuration of the apical epithelia, albeit in partial portions.

In the current study, we clearly elucidated the entire configuration of the apical epithelia of guinea pig premolars/molars using a 3D reconstruction method based on serial horizontal sections and overcame the disadvantages associated with SEM by applying KOH digestion. Furthermore, this method enabled us to determine the morphology of the apical epithelia within optimal sections, and to examine the apical epithelia from optimal angles by sectioning the 3D reconstructed epithelium in chosen planes (Figs. 5 and 6, Supplementary data 6-8). The apical epithelial components of the premolars/molars were M-shaped on the crown-analogue side and Δ-shaped on the root-analogue side. Two epithelial bulges (mesial and distal ABs) were located near the top of the M-shaped epithelium. Because one AB forms inverted U-shaped enamel on the crown-analogue side of mouse incisors [11,12], it is reasonable to assume that two (mesial and distal) ABs produce M-shaped enamel

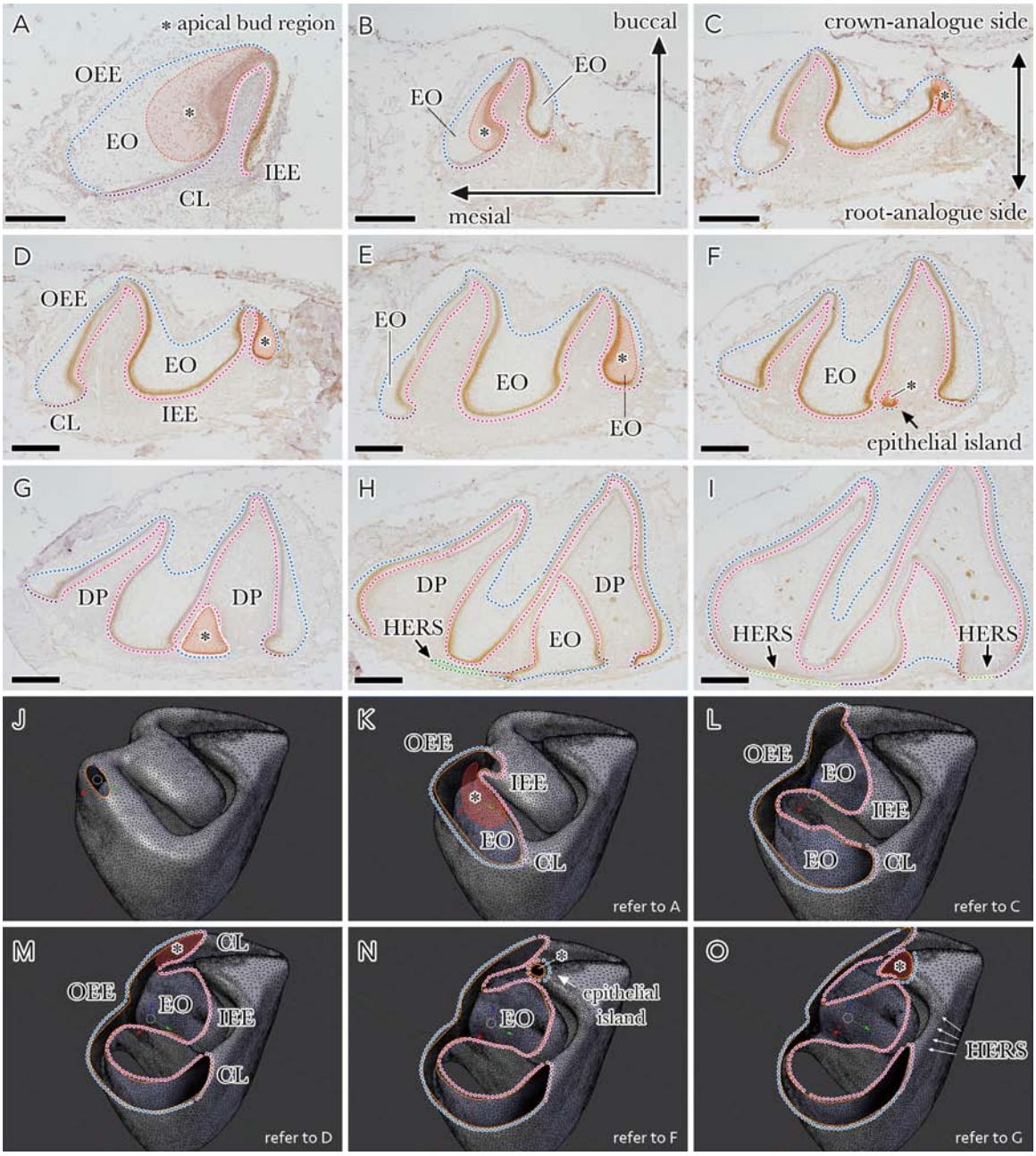

Fig. 3. Sox2-immunostained sections of the tooth germ. The figure illustrates Sox2-immunostained horizontally sliced paraffin sections of the tooth germ of the mandible first (E-I) and second (A-D) molars of 3-week-old guinea pigs at different positions, and 3D views (J-O) of the tooth germ ground at different positions (A, C, D, F, and G corresponding to K, L, M, N, and O, respectively). (A) There were intense reactions in the epithelial components (mesial AB) of the crown-analogue side. (B) This immunopositive reaction extended throughout the inner enamel epithelium (IEE). (C) There was another intense reaction within the epithelial components (distal AB) of the crown-analogue side. (D, E) This reaction also extended throughout the IEE. (F) An additional intense Sox2-immunopositive epithelial island (lingual AB in the mandible) appeared on the root-analogue side. (G) The boundary of this island continued as an intense staining pattern. The Sox2 immunoreactivity gradually decreased in intensity on the crown-analogue side, and the cervical loops (CLs) remained immunostained even as the sections approached the occlusal side. (H, I) Four Hertwig epithelial root sheaths (HERSs)—in which Sox2-positive cells intermingle with Sox2-negative cells—elongated mesiodistally from the mesial CL, the island CLs, and the distal CL to combine, resulting in the establishment of an epithelial covering surrounding the dental papilla on the root-analogue side. Bars = 500 μm (B-I), 250 μm (A). *apical bud (shaded area surrounded by a broken red line); CL, cervical loop (purple dotted lines); DP, dental pulp; EO, enamel organ; IEE; inner enamel epithelium (red dotted lines); OEE, outer enamel epithelium (blue dotted lines). (For interpretation of the references to color in this figure legend, the reader is referred to the web version of this article).

on the crown-analogue side of guinea pig premolars/molars. A large mushroom-like epithelial prominence in the valley of the M-shape may correspond to the merged area of two cervical loops. Furthermore, a Δ-shaped epithelial island appeared near the valley of the M-shaped epithelium, so that the S-shaped dental papilla was surrounded by M- and Δ-shaped epithelia on the crown- and root-analogue sides, respectively.

Supplementary material related to this article can be found online at https://doi.org/10.1016/j.job.2019.01.002.

4.2. Stem cell niche in the apical epithelium of guinea pig premolars/molars

In the present study, we identified the stem cell niche in the apical epithelium of the guinea pig premolars/molars by conducting an immunohistochemical investigation of Sox2. When we observed the serial Sox2-immunostained sections, there was an intense immunoreaction at the apical end of the ABs of the crown-analogue portion. Compared to the proliferation assay in our previous study

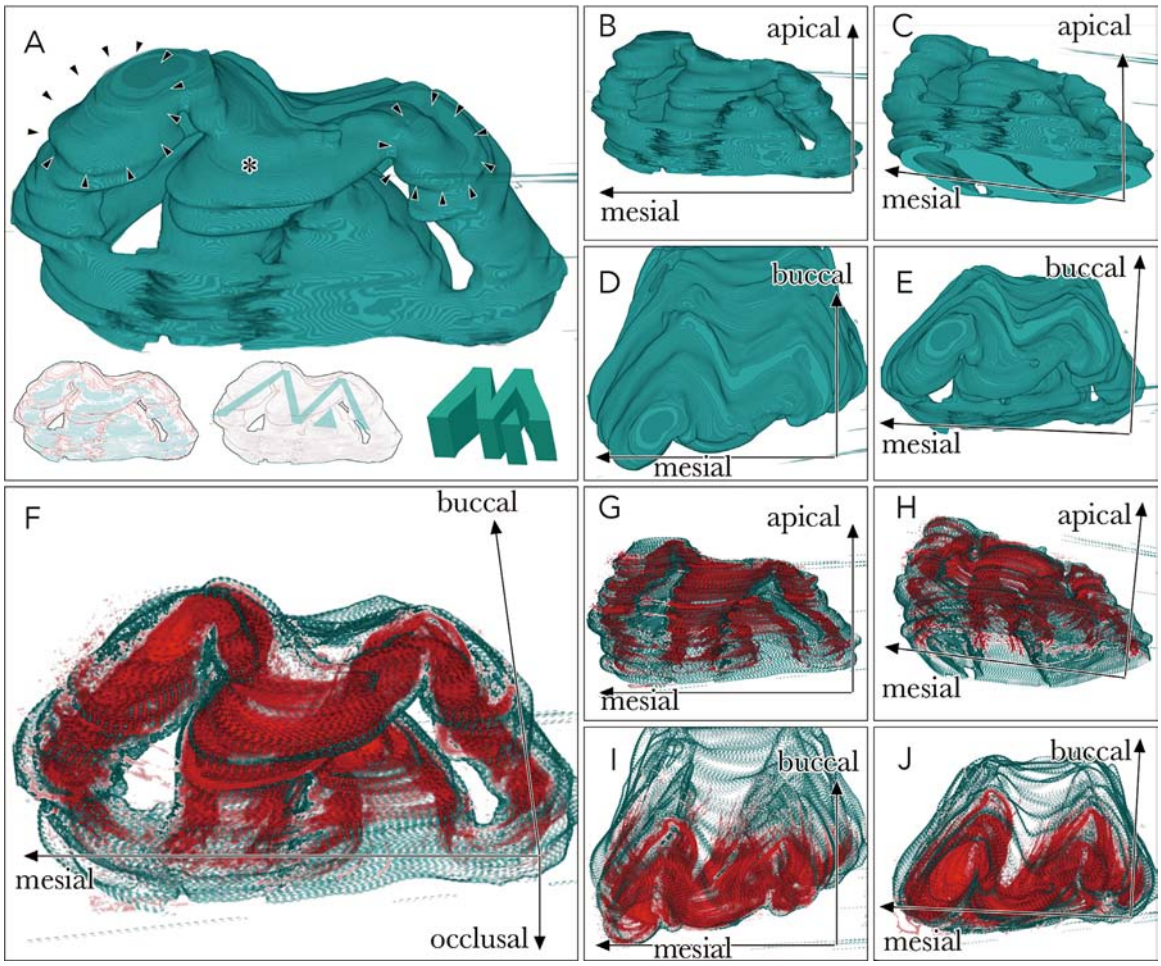

Fig. 4. Three-dimensional configuration of a mandible second molar. The figure represents the three-dimensional (3D) configuration of the apical epithelial tissue (A-E) of a guinea pig's mandible second molar, and the same tissue immunostained for Sox2 (F-J). (A-E) The apical epithelial components of the molar show the combined features of the M-shape on the crown-analogue side and the Δ-shape on the root-analogue side. Two epithelial bulges (mesial and distal ABs: arrowheads in A) are located near the tops of the M-shaped epithelium, and there is a large mushroom-like epithelial prominence (*) in the valley of the M-shape. A Δ-shaped epithelial island appeared near the valley of the M-shaped epithelium, so that the S-shaped dental papilla was surrounded by M- and Δ-shaped epithelia on the crown- and root-analogue sides, respectively. (F-J) The Sox2-positive reactions represented the combined features of the M- and Δ-shapes that corresponded to the ABs and IEE, and the Hertwig epithelial root sheaths (HERSs) and other components such as the stratum intermedium (SI), stellate reticulum (SR), and outer enamel epithelium (OEE) of the enamel organ showed evidence of disperse Sox2-positive reactions.

[20], the intensity attributable to Sox2 immunoreactivity decreased in the transit-amplifying (TA) cells, and disappeared in differentiated cells such as preameloblasts and ameloblasts. In contrast, there were Sox2 immunoreactions in the IEE, which connects the AB with the CL or HERS in the root-analogue dentin. These Sox2 immunoreactions persisted until the occlusal side, where Sox2-positive cells and proliferating cells intermingled in the CL and HERS, resulting in the persistence of Sox2 immunoreactions on the occlusal side compared to the crown-analogue dentin. In mouse incisors, Sox2 immunoreaction is apparent in the AB, and the IEE, OEE, and SI cells continue to produce positive reactions, but there is a dramatic reduction in the intensity attributable to Sox2-positive TA cells in the crown-analogue portion [22], and Sox2 immunoreactions diminish in the CL and HERS of the root-analogue region [16]. Sox2 immunoreactions are apparent in the crown-analogue portions of both mouse incisors and guinea pig premolars/molars, but there are differences in Sox2 immunoreactivity between mice and guinea pigs within the root-analogue regions.

4.3. Relationship between the morphology of continuously growing teeth and the number and arrangement of ABs

In the present study, we investigated both the 3D configuration of the apical epithelia of guinea pig premolars/molars and the 3D distribution of the Sox2-positive stem cell niche, which continuously supplies TA progenies. Based on the current findings, we propose a hypothesis regarding the relationship between the morphology of continuously growing teeth and the number and arrangement of their ABs. In mouse incisors, the Sox2-positive stem niche is restricted to the AB [16,22], and has a human head-like appearance [11]. Stem cell-derived TA progenies go through the sequential steps of exiting the niche, active proliferation, differentiation, and matrix deposition, and appear as a single cone from the perspective of a frontal section. The apical end of the postnatal incisor contains enamel knot-like structures, and expresses markers for enamel knots such as *Fgf4*, *Shh*, *Msx2*, and *P21* [12]. Therefore, we also propose a relationship between the number of enamel knots and crown morphogenesis. In a previous study, we reported that four ABs—mesial, distal, intercuspal, and lingual (or buccal)—exist in guinea pig premolars/molars [20]. Despite this finding, we must reconsider our hypothesis, because the present study demonstrates that there are no localized stem cell niches in the intercuspal epithelia of these teeth, and there are three ABs—mesial, distal, and lingual (or buccal)—in the apical end of the premolars/molars. These findings suggest that, in contrast to the single AB in mouse incisors, two ABs (mesial and distal) are arranged side by side, and the distal CL of the mesial AB

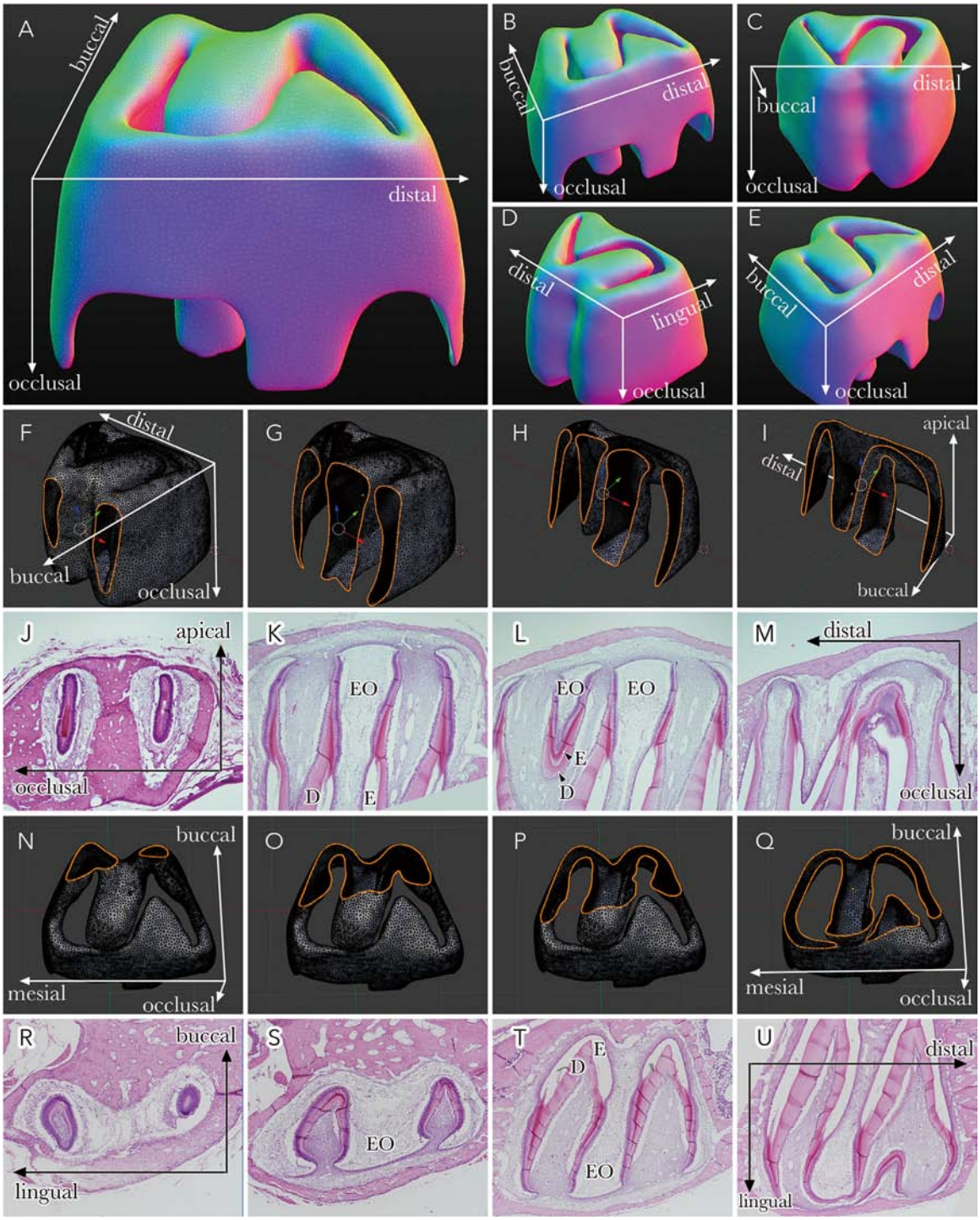

Fig. 5. Ideal 3D computer graphic of the apical epithelial tissue. The figure represents the ideal 3D computer graphic (CG) of the apical epithelial tissue (A-E), the same CG where the crown-analogue surface was sagittally (F-I) and horizontally (N-Q) trimmed at different positions corresponding to the sections bellow, and the actual hematoxylin and eosin (H&E)-stained sagittally (J-M) and horizontally (R-U) cut sections of the molars of a guinea pig. These CGs were artificially generated using Sculptris (released in 2011; Pixologic, Inc., CA, USA) (A-E) and Blender (ver. 2.79; Stichting Blender Foundation, Amsterdam, Netherlands) (F-I, N-Q) software packages. These CGs precisely reproduce the actual complex 3D features of the apical epithelial tissue.

and the mesial CL of the distal AB configure the intercuspal epithelia. Furthermore, there appears to be a lingual AB in the mandible and a buccal AB in the maxilla. However, we should note that a mesial or distal AB creates a concave morphology, whereas a lingual or buccal AB confers a convex appearance, resulting in the combination of two cusps and one concave cusp in the horizontal sections to create S-shaped dentin. In the root-analogue portion of the mouse incisors, each AB-derived mesial or lateral CL elongates in the lingual direction to become the HERS. These two HERSs fuse together and surround the dental papilla, resulting in the oval-shaped structure visible in the cross-section. In contrast, the mesial-AB-derived mesial CL and the distal-AB-derived distal CL become HERSs, elongate mesially and distally, and fuse with the lingual- or buccal-AB-derived HERS, forming root-analogue dentin covered with cementum on the lingual side of the mandible or the buccal side of the maxilla in the guinea pigs.

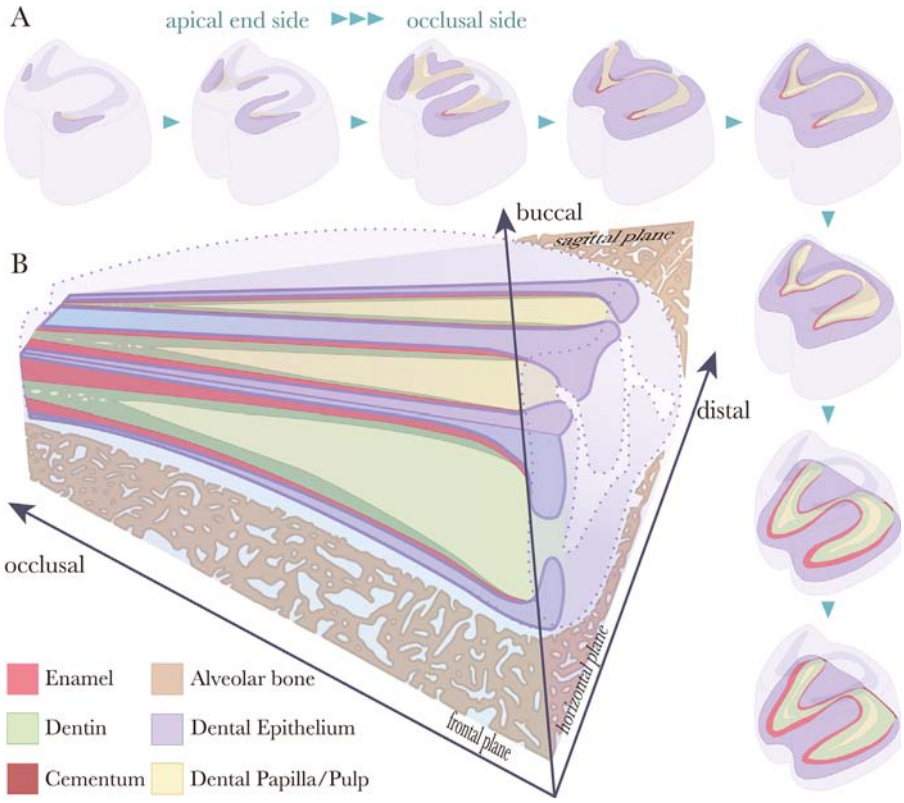

Fig. 6. Diagrams showing 3D views of a guinea pig premolar/molar. The diagrams show 3D views of a guinea pig premolar/molar trimmed frontally, sagittally (B), and horizontally (A).

5. Conclusions

In the present study, we used a 3D reconstruction method based on serial sections. The study demonstrated the morphological features of the apical epithelial components of premolars/molars. The combined features result in the M-shape on the crown-analogue side and the Δ-shape on the root-analogue side. We observed three Sox2-positive epithelial bulges on the tops of the M-shaped epithelia and the Δ-shaped epithelium. The Sox2-positive epithelial stem cell niches were restricted to the apical end of the crown-analogue side, whereas in the root-analogue region, the cell niche was sparsely distributed and extended to the occlusal side, including to the CL and HERS. These findings suggest that guinea pig cheek teeth have three ABs, and the complex configuration of these types of teeth can be attributed to the rapid formation of crown-analogue dentin followed by the long-term formation of root-analogue dentin.

Acknowledgments

The authors cordially thank Mr. Shinichi Kenmotsu for his technical assistance. This work was supported by a Grant-in-Aid for Scientific Research (B) (no. 17H04366 to H.O.) from the Japan Society for the Promotion of Science (JSPS).

Ethical approval

All of the animal experiments were conducted in compliance with a protocol that was reviewed by the Institutional Animal Care and Use Committee and approved by the President of Niigata University (SA00127).

Conflicts of interest

The authors declare no conflicts of interest with respect to the authorship and/or publication of this article.

Author contributions

Yuta Seino, data curation, investigation, methodology, validation, visualization, writing.

Mitsushiro Nakatomi, data curation, methodology, validation, writing - review & editing

Hiroko Ida-Yonemochi, methodology, validation, writing - review & editing

Daisuke Koga, methodology, validation, writing - review & editing

Tatsuo Ushiki, methodology, validation, writing - rewiew & editing

Hayato Ohshima, conceptualization, data curation, funding acquisition, supervision, validation, writing.

References

[1] Jernvall J, Thesleff I. Reiterative signaling and patterning during mammalian tooth morphogenesis. Mech Dev 2000;92:19–29.
[2] Bei M. Molecular genetics of tooth development. Curr Opin Genet Dev 2009;19:504–10.
[3] Tummers M, Thesleff I. The importance of signal pathway modulation in all aspects of tooth development. J Exp Zool B Mol Dev Evol 2009;312B:309–19.
[4] Cai J, Cho SW, Kim JY, Lee MJ, Cha YG, Jung HS. Patterning the size and number of tooth and its cusps. Dev Biol 2007;304:499–507.
[5] Li L, Tang Q, Nakamura T, Suh JG, Ohshima H, Jung HS. Fine tuning of Rac1 and RhoA alters cuspal shapes by remolding the cellular geometry. Sci Rep 2016;6:37828.
[6] Evans AR, Wilson GP, Fortelius M, Jernvall J. High-level similarity of dentitions

in carnivorans and rodents. Nature. 2007;445:78–81.
[7] Salazar-Ciudad I, Jernvall J. A gene network model accounting for development and evolution of mammalian teeth. Proc Natl Acad Sci USA 2002;99:8116–20.
[8] Salazar-Ciudad I, Jernvall J. A computational model of teeth and the developmental origins of morphological variation. Nature 2010;464:583–6.
[9] Smith CE, Warshawsky H. Cellular renewal in the enamel organ and the odontoblast layer of the rat incisor as followed by radioautography using 3H-thymidine. Anat Rec 1975;183:523–61.
[10] Ohshima H, Yoshida S. The relationship between odontoblasts and pulp capillaries in the process of enamel- and cementum-related dentin formation in rat incisors. Cell Tissue Res 1992;268:51–63.
[11] Harada H, Ohshima H. New perspectives on tooth development and the dental stem cell niche. Arch Histol Cytol 2004;67:1–11.
[12] Nakatomi C, Nakatomi M, Saito K, Harada H, Ohshima H. The enamel knot-like structure is eternally maintained in the apical bud of postnatal mouse incisors. Arch Oral Biol 2015;60:1122–30.
[13] Ohshima H, Nakasone N, Hashimoto E, Sakai H, Nakakura-Ohshima K, Harada H. The eternal tooth germ is formed at the apical end of continuously growing teeth. Arch Oral Biol 2005;50:153–7.
[14] Harada H, Kettunen P, Jung HS, Mustonen T, Wang YA, Thesleff I. Localization of putative stem cells in dental epithelium and their association with Notch and FGF signaling. J Cell Biol 1999;147:105–20.
[15] Smith CE. Cell turnover in the odontogenic organ of the rat incisor as visualized by graphic reconstructions following a single injection of 3H-thymidine. Am J Anat 1980;158:321–43.
[16] Juuri E, Saito K, Ahtiainen L, Seidel K, Tummers M, Hochedlinger K, Klein OD, Thesleff I, Michon F. Sox2+ stem cells contribute to all epithelial lineages of the tooth via Sfrp5+ progenitors. Dev Cell 2012;23:317–28.
[17] Seidel K, Ahn CP, Lyons D, Nee A, Ting K, Brownell I, Cao T, Carano RA, Curran T, Schober M, Fuchs E, Joyner A, Martin GR, de Sauvage FJ, Klein OD. Hedgehog signaling regulates the generation of ameloblast progenitors in the continuously growing mouse incisor. Development 2010;137:3753–61.
[18] Starkey WE. Continuous growth in the teeth of rabbits surveyed with tritiated thymidine and tritiated glycine. Br Dent J 1967;123:73–83.
[19] Tummers M, Thesleff I. Root or crown: a developmental choice orchestrated by the differential regulation of the epithelial stem cell niche in the tooth of two rodent species. Development 2003;130:1049–57.
[20] Hashimoto E, Nakakura-Ohshima K, Kenmotsu S, Suzuki H, Nakasone N, Saito C, Harada H, Ohshima H. The relationship between the cusp pattern and plural stem cell compartments in Guinea pig cheek teeth by chasing BrdU-labeling. Arch Histol Cytol 2008;71:317–32.
[21] Ushiki T, Murakumo M. Scanning electron microscopic studies of tissue elastin components exposed by a KOH-collagenase or simple KOH digestion method. Arch Histol Cytol 1991;54:427–36.
[22] Ishikawa Y, Nakatomi M, Ida-Yonemochi H, Ohshima H. Quiescent adult stem cells in murine teeth are regulated by Shh signaling. Cell Tissue Res 2017;369:497–512.